



Geophysical Research Letters

-

RESEARCH LETTER

10.1029/2025GL115215

Key Points:

- To understand the localized longlasting volcanism of the Moon, we developed a numerical model of magmatism in the convecting mantle
- Partially molten plumes ascend from the deep mantle to the uppermost level to cause the calculated volcanic activity
- Localized radioactive enrichment in the uppermost mantle maintains the plume activity for billions of years to cause volcanism

Supporting Information:

Supporting Information may be found in the online version of this article.

Correspondence to:

K. U, u-kenyo0822@g.ecc.u-tokyo.ac.jp

Citation:

U, K., Kameyama, M., Nishiyama, G., Miyagoshi, T., & Ogawa, M. (2025). Long-lasting volcanism of the Moon aided by the switch in dominant mechanisms of magma ascent: Role of localized radioactive enrichment in a numerical model of magmatism and mantle convection. *Geophysical Research Letters*, 52, e2025GL115215. https://doi.org/10.1029/2025GL115215

Received 4 FEB 2025 Accepted 30 MAR 2025

© 2025. The Author(s).

This is an open access article under the terms of the Creative Commons

Attribution License, which permits use, distribution and reproduction in any

medium, provided the original work is

properly cited.

Long-Lasting Volcanism of the Moon Aided by the Switch in Dominant Mechanisms of Magma Ascent: Role of Localized Radioactive Enrichment in a Numerical Model of Magmatism and Mantle Convection

Ken'yo U¹, Masanori Kameyama^{2,3}, Gaku Nishiyama^{4,5,6}, Takehiro Miyagoshi³, and Masaki Ogawa¹

¹Department of Earth Sciences and Astronomy, The University of Tokyo, Meguro, Japan, ²Geodynamics Research Center, Ehime University, Matsuyama, Japan, ³Japan Agency for Marine-Earth Science and Technology, Yokohama, Japan, ⁴German Aerospace Center, Institute of Planetary Research, Berlin, Germany, ⁵Department of Earth and Planetary Science, The University of Tokyo, Bunkyo, Japan, ⁶RISE Project, National Astronomical Observatory of Japan, Mitaka, Japan

Abstract Significant volcanic activity continued for billions of years since 3.5–4 Gyr ago in the Procellarum KREEP Terrane (PKT) of the Moon, but not so significant outside the PKT. To understand this volcanic history, we developed a 2-D numerical model of magmatism and mantle convection; the effects of the PKT on lunar evolution are considered by initially imposing a region of localized radioactive enrichment. The calculated volcanism is driven by two different mechanisms. Early volcanism occurs when magma generated in the deep mantle by internal heating ascends to the surface as partially molten plumes. The basaltic blobs in the uppermost mantle formed by this magmatism then sink into the deep mantle, triggering further plumes that cause a resurgence of volcanism in its later history. Our model suggests that later plumes caused by sinking basaltic blobs are the cause of the long-lasting volcanism in the PKT.

Plain Language Summary Geological observations of the Moon have revealed that active volcanism took place at 3–4 Gyr ago and continued for billions of years in the Procellarum KREEP Terrane (PKT), a region enriched in radioactive heat-producing elements (HPEs). Here, we calculated a 2-D model of magmatism and mantle convection, considering a locally HPE-enriched area (EA) beneath the crust to model this localized long-lasting volcanism in the PKT. Localized volcanism continues for billions of years owing to ascending partially molten plumes in our model. However, the mechanism of ascent of plumes changed with time. The early volcanic activity is caused by the ascent of partially molten plumes that are generated by strong internal heating at the base of the mantle. These plumes are globally distributed. The compositionally dense basaltic blobs in the uppermost mantle outside the EA, formed by the earlier magmatism, sink into the deep mantle, triggering counterflows that induce further partially molten plumes. These plumes cause volcanism above the EA from 1.2 to 2.8 Gyr. Our model suggests that the volcanism in the later stage caused by sinking basaltic blobs plays a crucial role in the long-lasting volcanism in the PKT.

1. Introduction

Understanding the volcanism of the Moon has been a long-standing issue in studies of lunar mantle evolution (e.g., Arai et al., 2008; Haupt et al., 2024; Head et al., 2023; Kirk & Stevenson, 1989; Solomon & Chaiken, 1976). Geological observations have revealed that volcanism has been particularly active in the Procellarum KREEP Terrane (PKT) located on the nearside, which is enriched in radioactive heat-producing elements (HPEs) (e.g., Jolliff et al., 2000; Kamata et al., 2013; Lawrence et al., 2000; Wieczorek & Phillips, 2000). Volcanism has occurred in other regions but has been less active (e.g., Shearer et al., 2006). In the PKT, volcanic activity continued for billions of years (e.g., Cho et al., 2012; Giguere et al., 2022; Kato et al., 2017; Morota et al., 2011) with a peak at 3.5–4 Gyr ago (e.g., Che et al., 2021; Hiesinger et al., 2000, 2003; Hurwitz et al., 2013; Nagaoka et al., 2020; Su et al., 2022; Whitten & Head, 2015). This period of active volcanism coincides with the time of the radial expansion of the Moon: the Moon expanded globally by 0.5–5 km until around 3.8 Gyr ago (e.g., Andrews-Hanna et al., 2013, 2014; Liang & Andrews-Hanna, 2022; Nishiyama et al., 2024; Sawada et al., 2016) and then contracted globally over time (Frueh et al., 2023; Yue et al., 2017), by around 1 km or less in the past 1 Gyr (e.g.,

Clark et al., 2017; Klimczak, 2015; Watters et al., 2010, 2015). To understand the long-lasting history of lunar volcanism, which mostly occurs in the PKT, we used a 2-D polar rectangular model of magmatism in the convecting lunar mantle (U et al., 2023b).

Various numerical models have been developed to account for the long-lasting volcanism of the Moon (e.g., Breuer & Moore, 2015; Solomon & Head, 1979; Wilson & Head, 2003). Some numerical models, in which the surface is covered by the HPE-enriched crust or a regolith layer as a blanket layer, suggest that magma persists in the uppermost mantle for 1-2 Gyr (e.g., Konrad & Spohn, 1997; Spohn et al., 2001; Ziethe et al., 2009). This partially molten region, however, extends globally and is unlikely to have caused the localized volcanism at the PKT. Some earlier researchers suggest that the localized volcanism is caused by one or some hot plumes growing from a layer of ilmenite-bearing cumulates (IBC) enriched in HPEs that developed on the core-mantle boundary (CMB) in the lunar early history (e.g., Stegman et al., 2003; de Vries et al., 2010; W. Zhang, Zhang, & Li, 2022; N. Zhang et al., 2013a, 2017; W. Zhang et al., 2023) owing to the magma ocean and mantle overturn (e.g., Hess & Parmentier, 1995; Ringwood & Kesson, 1976). Although the plume enriched in the IBC component ascends by thermal buoyancy in these models, it is unclear if the large excess density of the IBC component, as expected from earlier models of mantle overturn, allows the ascent of such a compositionally dense plume in the Moon (e.g., Le Bars & Davaille, 2004; H. Li et al., 2019; Yu et al., 2019; Zhao et al., 2019). On the other hand, Wieczorek and Phillips (2000) and Laneuville et al. (2013, 2018) assumed a locally HPE-enriched area (called EA hereinafter) at the top of the mantle in the initial condition and found that the area remained partially molten for more than 3 Gyr. Various mechanisms have been suggested for the EA formation: differences in crystallization rates between the hemispheres of the lunar magma ocean (Loper & Werner, 2002; Wasson & Warren, 1980); the residual layer enriched in KREEP (K, rare earth elements, and P-rich material) after the mantle overturn (e.g., Parmentier et al., 2002; N. Zhang, Ding, et al., 2022); impact-induced convection (e.g., Rolf et al., 2017; Zhu et al., 2019; N. Zhang, Ding, et al., 2022; Jones et al., 2022). In the models of the subsequent thermal evolution of the mantle, however, the extraction of HPEs from the partially molten area by segregating magma (Cassen et al., 1979; Cassen & Reynolds, 1973) is neglected, and HPEs remain in the uppermost mantle throughout the calculated 3 Gyr. Ogawa (2018a) found that partially molten regions solidify within 2 Gyr when HPE-extraction by magmatism is considered.

To understand the mantle evolution of the Moon, constrained by its volcanic history as well as radial expansion/contraction history, we extend the 2-D model of magmatism and mantle convection that we have developed (U et al., 2023b). In this model, magma is generated by decompression melting and internal heating, then migrates upward in partially molten regions as a permeable flow through the coexisting matrix; thermal, compositional, and melt buoyancy drive mantle convection in a Newtonian fluid with temperature-dependent viscosity; heat, mass, and incompatible HPEs are transported by magma. In our earlier study, we initiated the calculation with a compositionally stratified mantle, enriched with the IBC component at the base of the mantle (U et al., 2023b) following earlier studies of the magma ocean: during the last stage of crystallization of the lunar magma ocean, a dense IBC layer enriched in KREEP develops at the top of the mantle and subsequently sinks to the CMB, a process called mantle overturn (e.g., Alley & Parmentier, 1998; Boukaré et al., 2018; Hess & Parmentier, 1995). In addition to this initial stratification, we also consider a localized enrichment of HPEs beneath the crust to model the PKT and investigate whether this EA induces a localized volcanism similar to that observed at the PKT (Figure 1a).

2. Model Descriptions

We used a 2-D annular model of mantle convection and magmatism, developed by U et al. (2023b). The finite difference numerical code calculates the energy, mass and momentum conservation equations of mantle convection in $R = [(r,\theta)| 385 \text{ km} \le r \le 1735 \text{ km}, \ 0 \le \theta \le \pi]$ on a mesh with 128 (radial direction) times 256 (lateral direction) mesh points, under the Boussinesq approximation (See Text S1-1 in Supporting Information S1 for the detail of the basic equations). To model the blanket effect of the crust (Ziethe et al., 2009), we reduced thermal diffusivity by a factor of two within a 35 km-thick blanket layer at the top of the mantle. The core is modeled as a heat bath with a uniform temperature (see Equations S20, S21 in Text S1-1 in Supporting Information S1). The vertical sidewalls are insulated, while the surface boundary is fixed at 270 K; all boundaries are shear stress-free and impermeable to both magma and matrix.

U ET AL. 2 of 12

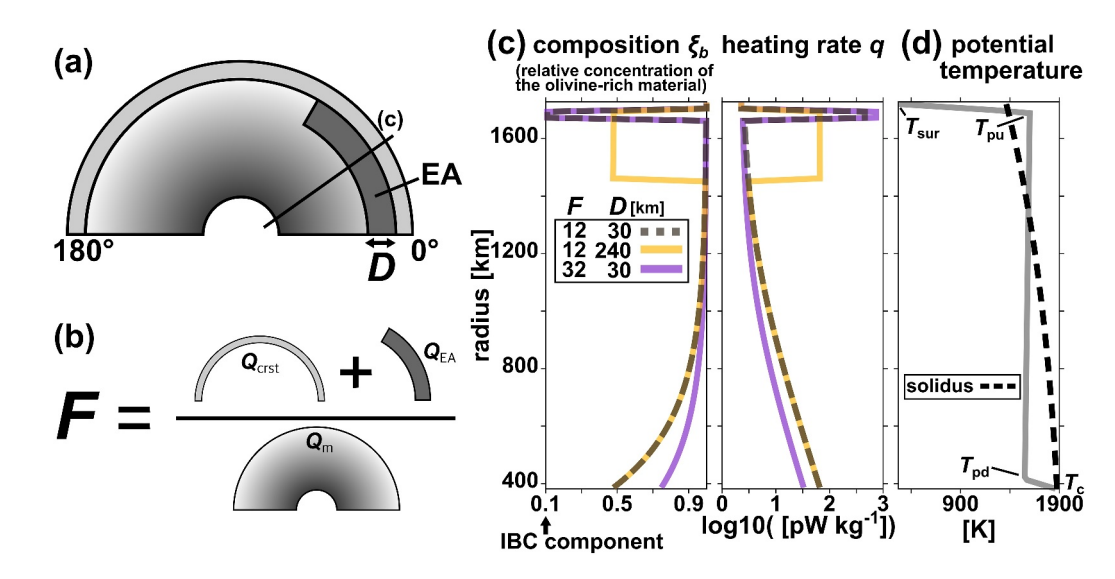


Figure 1. (a, b) An illustration of the initial distribution of heat-producing elements (HPEs). The distribution is laterally uniform except for the enriched area "EA." In (b) F is the ratio of the total amount of HPEs in the crust $Q_{\rm crst}$ and the EA $Q_{\rm EA}$ to that in the mantle $Q_{\rm m}$ (see Texts S1-2 in Supporting Information S1). Also shown are (c) the initial distribution of the composition and heating rate along the line in (a); (d) the initial distribution of the potential temperature ($T_{\rm sur} = 270~{\rm K}$, $T_{\rm pu} = 1,600~{\rm K}$, $T_{\rm pd} = 1,550~{\rm K}$, and $T_{\rm c} = 1,875~{\rm K}$ are assumed in this figure).

The convecting material is a binary eutectic system $(A_{\xi}B_{1-\xi})$ composed of an olivine-rich material (A_1B_0) with a density of 3,300 kg m⁻³ and an IBC material (A_0B_1) with a density of 3,745 kg m⁻³ (e.g., Elkins-Tanton et al., 2011; Liang et al., 2024; Snyder et al., 1992). The concentration of the olivine component is denoted by ξ , then Equation 1 below would give the concentration of the olivine-rich material in the partially molten mantle. The eutectic composition is at $\xi_e = 0.1$ $(A_{0.1}B_{0.9})$. We adopted this simple binary material as a model of mantle materials to mimic variation in density distribution in the mantle caused by segregation of compositionally dense basaltic materials by magmatism; a detailed petrologic simulation of the mantle is beyond the scope of this study. The bulk composition ξ , that is, the relative concentration of olivine-rich material, is calculated from the composition of the solid phase ξ_s and that of the liquid phase ξ_1 written as

$$\xi = (1 - \phi)\xi_s + \phi\xi_1,\tag{1}$$

where ϕ is the melt-content. The solidus and liquidus temperatures are calculated from the phase diagram assumed for the binary eutectic system (see Equations S9–S11 and S17–S19 in Text S1-1 in Supporting Information S1). The convecting material contains HPEs that decay with time. Magmatism is modeled by the generation and upward migration of magma as a permeable flow (e.g., McKenzie, 1984; Miller et al., 2014). The flow is driven by the buoyancy of magma, and the relative velocity between the velocity of melt \mathbf{u} and that of matrix \mathbf{U} is calculated from

$$\mathbf{u}^* - \mathbf{U}^* = -Mg^* \frac{\phi^2}{\phi_0^3} (\rho_s^* - \rho_l^*) \mathbf{e_r}, \tag{2}$$

where the asterisks stand for normalized quantities; $\mathbf{e_r}$ is the unit vector in the radial direction. $\rho_s - \rho_l$ is the density difference between solid and melt phases calculated as

$$\rho_{s}^{*} - \rho_{l}^{*} = \beta(\xi_{l} - \xi_{s}) + \frac{\Delta V_{l}}{V_{0}} [1 + \beta(1 - \xi_{l})]$$
(3)

(See Equations S6 and S7 in Supporting Information S1). Here, g is the gravitational acceleration; $\phi_0 = 0.05$ is the reference melt-content; $\Delta V_1/V_0$ is the amount of density reduction (see Equation S11 in Text S1-1 in Supporting Information S1). We assumed the reference permeability M to be

U ET AL. 3 of 12

$$M \equiv \frac{k_{\phi_0} \rho_0 g_0 L}{\kappa \eta_{\text{melt}}} \simeq 100, \tag{4}$$

where the parameter values are listed in Table S1 in Supporting Information S1. $\beta = 0.135$ is a constant that expresses the sensitivity of density to the bulk composition (see Text S1-1 in Supporting Information S1). In most cases, we assumed that the crustal density is higher than the density of magma for simplicity. However, the density of the lunar crust is lower than that of basaltic magma (e.g., Head & Wilson, 2017, 2020; Morota et al., 2009; Taguchi et al., 2017; Wilson & Head, 2017), and Lourenço et al. (2018) suggest that the thermal history of the Moon can substantially depend on the crustal density inversion. To clarify the effect of the density inversion, we increased the value of β to 0.253 in the blanket layer in a case (Case crst-F12-D30): the crustal density is 2,550 kg m⁻³ (Wieczorek et al., 2013) which is lower than the density of the basaltic magma at this value of β .

To simulate the localized enrichment of HPEs in the mantle beneath the PKT, we assumed the EA in $[(r,\theta)|\ 1700-D\ \mathrm{km}\le r\le 1700\ \mathrm{km},\ 0\le\theta\le 1/3\ \pi]$ that is enriched in HPEs and the IBC component, as illustrated in Figure 1a. We examined the dependence of calculated volcanism on the thickness of the EA "D" and on the ratio of the total amount of HPEs in the crust and the EA to the mantle "F" (Figures 1a and 1b); note that HPE-content in the crust is constant for simplicity (see Text S1-2 in Supporting Information S1). The searched range of "D" (10–240 km) is estimated from the thickness of the KREEP layer that remains after the mantle overturn (e.g., Charlier et al., 2018; Laneuville et al., 2013; Schwinger & Breuer, 2022; N. Zhang, Ding, et al., 2022). We also take the searched range of "F" (4–32) from previous estimates of Th concentrations in the enriched area (e.g., Laneuville et al., 2018; Wieczorek & Phillips, 2000); the upper value of the Th concentration is around the average surface composition shown by orbital gamma-ray spectroscopy data (e.g., Taylor & Wieczorek, 2014).

In the initial condition, we assumed that the mantle is compositionally stratified to simulate the stratification of the lunar mantle inferred from previous studies of the magma ocean and mantle overturn (e.g., Hess & Parmentier, 1995; Zhao et al., 2019). The contents of HPEs and the IBC component increase exponentially with depth while the content of the olivine-rich material decreases with depth (Figure 1c). The average of the internal heating rate over the entire mantle is fixed at $q_0 = 14.7 \, \mathrm{pW} \, \mathrm{kg}^{-1}$ at 4.4 Gyr ago as estimated from Table S2 in Text S1-1 in Supporting Information S1 for all the cases listed in Table S3 in Supporting Information S1. The potential temperature distribution in the initial condition (Figure 1d) is also taken from earlier models of the lunar mantle overturn (e.g., Boukaré et al., 2018; Yu et al., 2019) and the evolution model (U et al., 2022). The details of the initial condition are described in Text S1-2 in Supporting Information S1. Note that the uppermost mantle is partially molten in the initial condition (Figure 1d). This region persists for around 600 Myr (see Figure 2 below). However, the melt-content is small, up to only 1%, and this region does not affect the overall dynamics of the calculated mantle as we will describe below.

3. Results

In Figures 2 and 3 as well as the animation (Movie S1), we present the evolution of the mantle calculated in Case F12-D30 where F = 12 and D = 30 km (see also figures in Supporting Information S1).

Magma is generated in the deep mantle owing to the strong internal heating assumed in the initial condition (Figure 1c) and migrates upward as partially molten plumes to reach the uppermost mantle within the first 0.7 Gyr (Figures 2b and 2c; see also Figure S1a in Supporting Information S1); melt buoyancy is the main driving force of this flow. Magma rises to the depth level of 100 km beneath the EA in $[0 \le \theta \le 1/3 \pi]$, which is shallower than beneath the area outside the EA (Figures 3a and 3b; see also Figures S1b and S1c in Supporting Information S1). This is because the lithosphere is thinned beneath the EA owing to the strong heating by HPEs in the EA (Figures 2a and 2c; see also Figure S2 in Supporting Information S1). The magma transports HPEs and the basaltic component to the uppermost mantle, forming basaltic blobs (see the arrows in Figure 2d for 0.76 Gyr). A deeper part of the compositionally dense basaltic blobs eventually founders to the CMB as magma accumulates and the blobs grow (see the arrow in Figure 2d for 1.12 Gyr; see also the description in Text S2-1 in Supporting Information S1). The descending basaltic blobs trigger further ascent of partially molten plumes from the deep mantle driven by melt buoyancy, as depicted by the arrows in Figure 2b. Accordingly, the upward magma flux

U ET AL. 4 of 12

19448007, 2025, 8, Downloaded from https://agupubs.onlinelibrary.wiley.com/doi/10.1029/2025GL115215 by Dxch Zentrum F. Luft-U. Raum Fahrt In D. Helmholtz Geneim, Wiley Online Library on [24/11/2025]. See the Terms

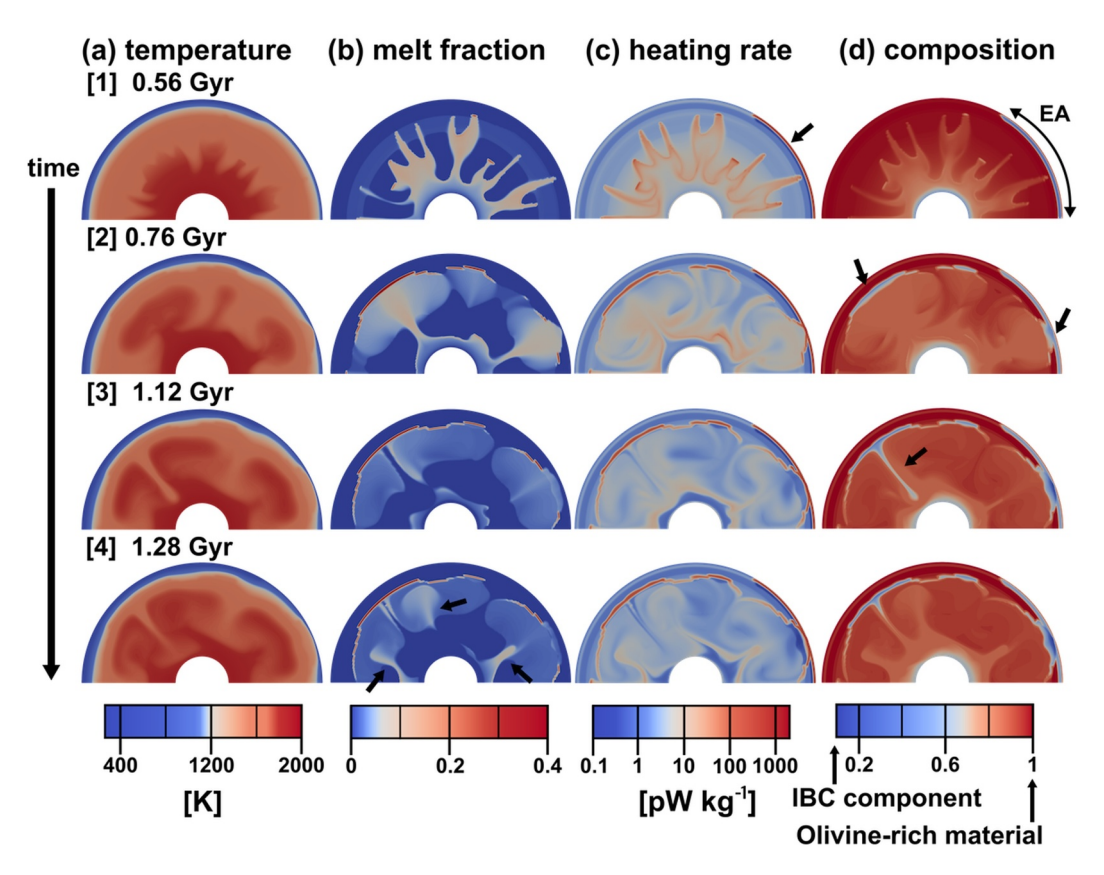


Figure 2. Snapshots of the distributions of (a) temperature, (b) melt-content, (c) internal heating rate, and (d) bulk composition calculated for the reference case (F = 12 and D = 30 km; Case F12-D30). The elapsed times are indicated in the figure. In (d), the blue color stands for the basaltic composition enriched in the IBC component, while the red color stands for the olivine-rich end-member. The numbers [1]–[4] correspond to those of Figure 3b.

beneath the EA becomes significant again from 1.2 to 2.8 Gyr (Figure 3b). The resurgence of magma flux is not found in our earlier models that are devoid of the EA (see the gray dotted line in Figure 3b). In contrast, the magma flux is negligibly small throughout the calculated history outside the EA due to the thicker lithosphere (Figures 3a and 3b). After 2.8 Gyr, the partially molten region in the mantle shrinks with time due to the decay of HPEs but persists until 4.4 Gyr (Movie S1 as well as Figure S1d in Supporting Information S1). From further numerical experiments with various values of D in the range of 10–240 km and F in the range of 4–32, we found that the localized volcanism continues for more than 1.5 Gyr in the cases with D < 120 km and 8 < F < 24 (see Text S2-2 in Supporting Information S1) including Table S3 and Figures S3, S4 in Supporting Information S1).

The resurgence of magma flux beneath the EA observed in the reference case is more pronounced in Case crst-F12-D30 where the crustal density is lower than the density of the basaltic magma (see Figures 3c, 3d and Figure S5 in Supporting Information S1). The upward magma flux shown in Figure 3c is substantial beneath the entire EA until 3.7 Gyr, and magma enriched in HPEs remains along the crust-mantle boundary even at as late as 3.5 Gyr (Figure S5 in Supporting Information S1). The resurgence of magma flux is so significant in crst-F12-D30 because the lower density of the crust prevents magma from transporting HPEs to the surface; HPEs remain beneath the crust to keep the lithosphere beneath the EA thinner compared with that in the reference case. The thinner lithosphere beneath the EA allows the magma generated by the counterflows to rise higher than that in the reference case; the magma flux increases locally several times when the heads of partially molten plumes ascend to the base of the crust (see Figures 3c and 3d; see also Figure S5 in Supporting Information S1 and Movie S2).

We found that strong internal heating and compositionally high density in the EA, as well as the existence of an initial mantle stratification, are important for the resurgence of magma flux beneath the EA (see Figures S6–S9 in Supporting Information S1). The resurgence of magma flux is not observed in Case noHeat-F12-D30 where the enrichment of HPEs in the EA is not considered (Figures S6a and S7 in Supporting Information S1). The

U ET AL. 5 of 12

19448007, 2025, 8, Downloaded from https://agupubs.onlinelibrary.wiley.com/doi/10.1029/2025GL115215 by Disch Zentrum F. Luft-U. Raum Fahrt In D. Helmholtz Gemein., Wiley Online Library on [24/11/2025]. See the Terms and Conditions (https://

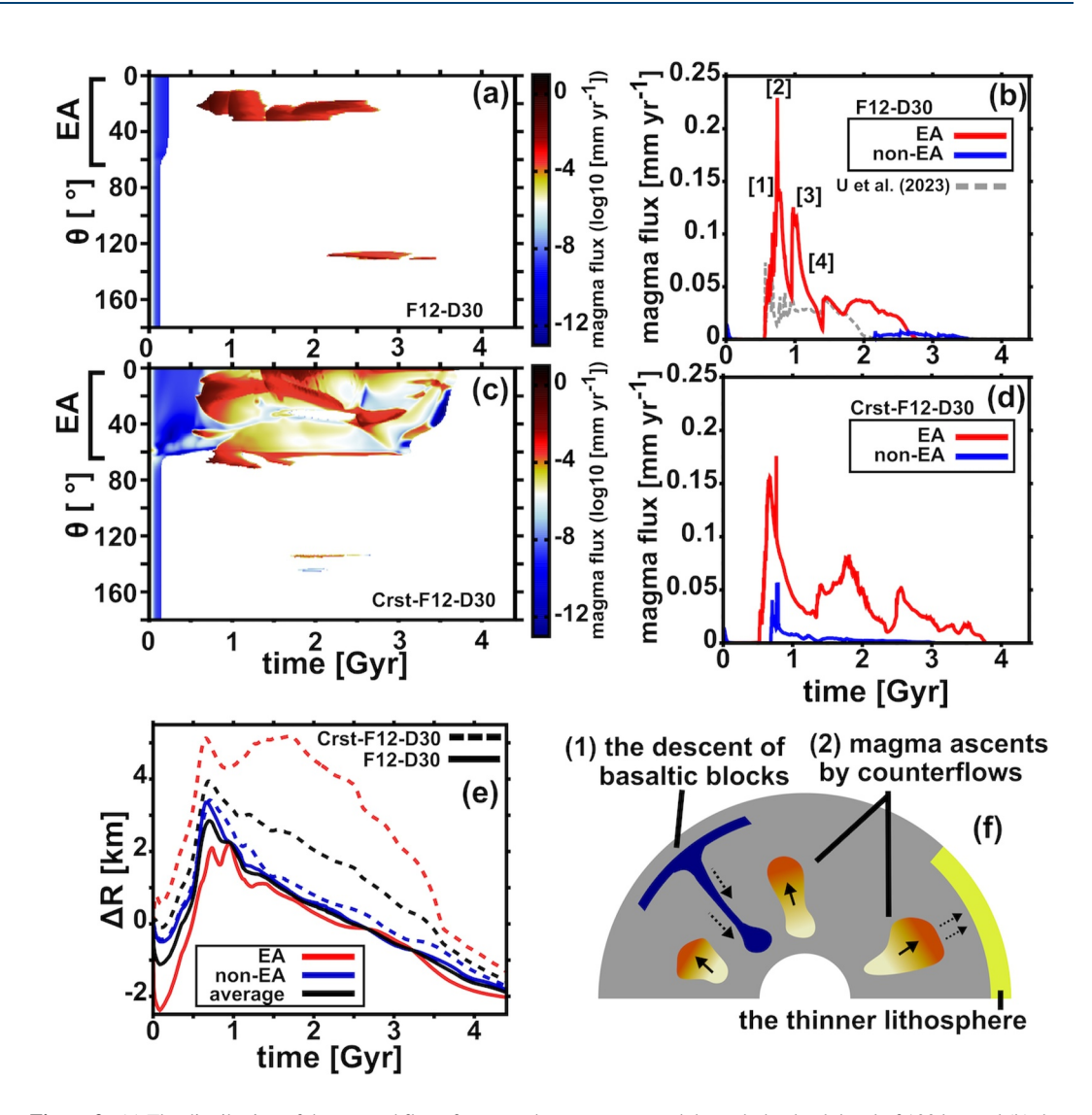


Figure 3. (a) The distribution of the upward flux of magma that passes upward through the depth level of 100 km and (b) the average flux of magma around the EA (the red line) and outside the EA (the blue line) at the depth level of 100 km in Case F12-D30 (the reference case). Also shown are (c and d) the magma flux calculated in Case crst-F12-D30 where the crust is less dense than basaltic magma; (e) the history of radius change ΔR calculated by Equation S24 in Text S1-3 in Supporting Information S1; (f) a schematic illustration of long-lasting volcanism with a couple of peaks in the PKT calculated in the model. In (b, d, and e), the blue lines and red lines stand for the average values in $[0 \le \theta \le 1/3 \pi]$ (beneath the EA) and in $[1/3 \pi < \theta \le \pi]$ (outside the EA), respectively, while the black lines stand for the total average values in $[0 \le \theta \le \pi]$. In (b), the gray line shows the magma flux in our earlier model (U et al., 2023b) where the EA is not considered (other parameters are the same as those assumed in Case F12-D30); the numbers [1]-[4] correspond to those of Figure 2.

resurgence occurs only briefly in Case noBa-F12-D30 where the compositional high density in the EA is not considered (Figures S6b and S8 in Supporting Information S1). This is due to the smaller density difference between the mantle and magma $\rho_s - \rho_l$ in the EA compared to the reference case, resulting in a lower permeable flow (Equations 2 and 3). On the other hand, magma flux at the depth level of 100 km is not observed since 0.5 Gyr after the start of the calculation in Case noStra-F12-D30 where the HPEs and the composition ξ are vertically uniform in the initial mantle (Figures S6c and S9 in Supporting Information S1). The deep mantle is not enriched in HPEs in this case, and the amount of generated magma is too small to let plumes ascend to the uppermost mantle. Magmatism caused by partially molten plumes does not occur at the Rayleigh number $Ra \le 2 \times 10^5$ (see Equation S3 and Text S2-4 in Supporting Information S1 which includes Movie S3 and Figures S10, S11 in Supporting Information S1) but continues for billions of years beneath the EA at $Ra \simeq 2 \times 10^6$ (Figures 3a and 3b). In contrast, the overall features of mantle evolution are not influenced by the

U ET AL. 6 of 12

value of the sensitivity of viscosity to temperature E_T (see Equation S4 and Text S2-4 in Supporting Information S1 including Figure S12 in Supporting Information S1). These parameter dependencies of the numerical results are the same as those shown in U et al. (2023b).

Figure 3e shows that the Moon expands globally by more than 3 km for the first 0.7 Gyr of the calculated history and then contracts at a rate of around -1 km Gyr⁻¹ in the past 1 Gyr in the reference case. The decomposition of radius change ΔR into the component caused by melting/solidification and by thermal expansion/contraction shows that the expansion is mainly caused by melting, while the contraction is mainly caused by thermal contraction (Figure S13 in Supporting Information S1). The overall feature of the radius change is not affected by the crustal density (see the black dotted line in Figure 3e). However, there is a drop in the radius beneath the EA $\Delta R_{\rm EA}$ at around 3.7 Gyr due to the solidification of the mantle in Case crst-F12-D30 (see Figure S14 in Supporting Information S1). This is because a partially molten region that persists until that time along the crust-mantle boundary beneath the EA solidifies (Figure 3c; see also Figure S5 in Supporting Information S1).

4. Discussions

Figure 3f illustrates how an EA causes a long-lasting volcanism in our models. In the earlier stage of mantle evolution, magma is generated in the deep mantle by internal heating and ascends to the uppermost mantle as partially molten plumes. In the area beneath the EA, magma rises to a shallower depth than in the area outside the EA because the lithosphere there is thinner owing to the strong internal heating assumed in the initial condition. This magmatism results in the formation of basaltic blobs beneath the lithosphere. The basaltic blobs outside the EA eventually sink to the CMB, triggering further plume activity that causes a long-lasting volcanism.

4.1. Comparison With Earlier Models of Lunar Volcanic History

A comparison with earlier mantle convection models of lunar volcanic history, which mostly occurs in the PKT and its surrounding area, shows the crucial role of melt buoyancy in our models. Some models suggest that localized volcanism is caused by thermal plumes from an HPE-enriched IBC layer on the CMB (e.g., N. Zhang et al., 2013b; Zhong et al., 2000). In these models, however, the compositional density contrast between the basal IBC layer and the overlying olivine-rich mantle is substantially less than 160 kg m⁻³ (see Figure 6 in H. Li et al. (2019)), the value suggested from some recent mantle overturn models (e.g., Maurice et al., 2024; Yu et al., 2019; Zhao et al., 2019). At this density contrast, the basal layer remains convectively stable and does not rise as a plume by thermal buoyancy alone (de Vries et al., 2010; Le Bars & Davaille, 2004). In contrast, a large fraction, around 60%, of the IBC component in the deep mantle arises as partially molten plumes mostly driven by melt buoyancy in our models (Figure 2) although the density contrast is more than 200 kg m⁻³ in our reference case (Figure 1c).

Our models also suggest the reason why volcanism continues so long in the PKT. In some of earlier models, a locally HPE-enriched area at the top of the mantle assumed in the initial condition remains partially molten for more than 3 Gyr (Laneuville et al., 2013, 2018; Wieczorek & Phillips, 2000). HPE-extraction from the enriched area by magmatism is, however, neglected in these models as we discussed before. In our models, magmatism continues long despite that HPE-transport by magma is taken into account, because the basaltic blobs formed by early magmatism descend to the CMB to trigger further ascent of partially molten plumes (Figures 2, 3a, and 3f). Besides, the melting history of the uppermost mantle depends on the crustal density. In Case crst-F12-D30 where the crustal density is lower than the density of the basaltic magma, HPEs are not extracted to the surface but remain at the base of the crust (see Figure S5 in Supporting Information S1). The HPEs at the crust-mantle boundary keep the lithosphere thin enough for revived plume activity to cause volcanism. The resurgence of magma flux is so significant beneath the entire EA for more than 3.5 Gyr due to the plume activity (Figures 3c and 3d). By comparing magma flux under varying initial conditions (Figures S6–S9 in Supporting Information S1), our simulations also show that both the initial mantle stratification and the EA beneath the crust play crucial roles in the resurgence of volcanism after 1 Gyr. The resurgence of the magma flux is observed in all of the cases with $Ra \simeq 2 \times 10^6$ regardless of the values of E_T (Figures S10–S12 in Supporting Information S1 as well as Movie S3) because the Rayleigh number Ra is high enough for partially molten plumes to grow. Note that a detailed discussion of volcanic history is possible in our models because we calculate the magma flux directly, rather than estimating it from the distribution of magma in the mantle, as is done in earlier models (e.g., Konrad & Spohn, 1997; Solomon & Toksöz, 1973; U et al., 2022; Wood, 1972).

U ET AL. 7 of 12

4.2. Comparison With the Observed Features of the Moon

The magma flux beneath the EA shown in our reference case is consistent with the observed history of volcanism in the PKT. Magma generated at depth by strong internal heating rises (Figure 2 for 0.56 and 0.76 Gyr), causing the peak of volcanism at 3.5–4 Gyr ago (e.g., Hiesinger et al., 2000; Whitten & Head, 2015). The resurgence of volcanism triggered by the descending basaltic blobs is consistent with the observed long-lasting volcanic history in the PKT (e.g., Cho et al., 2012; Tian et al., 2023). The early expansion and later contraction of the Moon in the reference case (Figure 3e) are also consistent with those suggested from gravity gradiometry data and tectonic features (e.g., Andrews-Hanna et al., 2013; Matsuyama et al., 2021; van der Bogert et al., 2018). The plumes triggered by descending basaltic blobs are depleted in HPEs compared to the plumes that ascend in the early history (see the frames of 0.76 and 1.28 Gyr in Figures 2c and 2d; see also the animation). The plume activity in the later history can account for the HPE-depleted young basalts observed in the PKT (Che et al., 2021; Q.-L. Li et al., 2021; Su et al., 2022). It is, however, difficult to account for the temporal trend of increasing Ti content in the HPE-depleted mare basalts in the PKT after around 2.3 Gyr ago (Kato et al., 2017; Sato et al., 2017; D. Zhang, Su, et al., 2022). This trend may be due to the remelting of basaltic blobs in the uppermost mantle by the plumes that rise later (Figure 2). To understand this trend clearly, it is necessary to model magma evolution carefully, considering fractional crystallization (e.g., Luo et al., 2023).

Further calculations in a 3-D spherical mantle are important to more quantitatively predict the history of magma flux, radial expansion/contraction, and thermal history of the Moon and to compare the predictions with such observations as the temperature distribution in the Moon (e.g., Khan et al., 2006, 2014). As already found by Guerrero et al. (2018) for the Moon, 2-D polar rectangular models of mantle convection tend to predict higher average mantle temperatures compared to 3-D spherical models, especially when the core size is small. In the reference case, the mid-mantle temperature at 4.4 Gyr is about 100 K higher than current lunar estimates (Figure S1d in Supporting Information S1), which may result from the geometry of the convecting vessel.

5. Conclusions

To understand the long-lasting localized volcanism for billions of years in the PKT (the Procellarum KREEP terrane), we numerically simulated a 2-D polar rectangular model of magmatism and mantle convection where a localized heat-producing elements (HPEs) enrichment beneath the crust, called enriched area (EA) is considered to model the PKT in the initial mantle stratification (Figure 1).

Our simulations show that the localized volcanism, which continued for billions of years, is induced by ascent of partially molten plumes driven by two mechanisms. The early volcanism occurs as partially molten plumes ascend from the deep mantle owing to internal heating there (Figures 2 and 3b). Magma ascends to the uppermost mantle beneath the EA because the lithosphere there is thinned by the strong internal heating in the EA. The later activity of volcanism, in contrast, is caused by the counterflows of sinking basaltic blobs that are formed beneath the lithospheric lid outside the EA by the earlier magmatism; a deeper part of the compositionally dense basaltic blobs sinks into the deep mantle, triggering further magma ascent beneath the EA from 1.2 to 2.8 Gyr (Figures 3b and 3f). We found that the mantle evolves as illustrated in Figure 3f when the thickness of the EA is D < 120 km and the ratio of the total amount of HPEs in the crust and the EA to the mantle is 8 < F < 24 (see Figures S3, S4, and Table S3 in Supporting Information S1). Our models suggest that material transport and melt buoyancy by magmatism play critical roles in the lunar mantle evolution. In particular, the resurgence of volcanism in the later stage is important to account for the long-lasting volcanism in the PKT.

Data Availability Statement

The original data in all cases plotted in Table S3 in Supporting Information S1 and the numerical code used in this work are found at U et al. (2023a, 2024), respectively.

References

Alley, K. M., & Parmentier, E. M. (1998). Numerical experiments on thermal convection in a chemically stratified viscous fluid heated from below: Implications for a model of lunar evolution. *Physics of the Earth and Planetary Interiors*, 108(1), 15–32. https://doi.org/10.1016/S0031-9201(98)00096-X

Andrews-Hanna, J. C., Asmar, S. W., Head, J. W., III., Kiefer, W. S., Konopliv, A. S., Lemoine, F. G., et al. (2013). Ancient igneous intrusions and early expansion of the Moon revealed by grail gravity gradiometry. *Science*, 339(6120), 675–678. https://doi.org/10.1126/science.1231753

Acknowledgments The manuscript was greatly improved by the comments of the editor Kevin Lewis and two anonymous reviewers; the authors thank the editor and reviewers for their insightful suggestions. The authors would like to extend their sincere appreciation to M. Kayama at the University of Tokyo and T. Yanagisawa at JAMSTEC for their constructive comments. This work was supported by JST SPRING Grant JP-MJSP2108 and JSPS KAKENHI Grant JP202412823 of Japan. This work was also supported by: the Joint Usage/Research Center PRIUS at Ehime University, the Earth Simulator of Japan Agency for Marine-Earth Science and Technology (JAMSTEC), "Exploratory Challenge on Post-K Computer" (Elucidation of the Birth of Exoplanets [Second Earth] and the Environmental Variations of Planets in the Solar System), and "Program for Promoting Research on the Supercomputer Fugaku" (Toward a unified view of the universe: from large scale structures to planets). This work used computational resources of the supercomputer Fugaku provided by the RIKEN Center for Computational Science through the HPCI System Research Project (Project ID: hp230204, hp240219). Animations and some figures were drawn with the ParaView by Sandia National Laboratory, Kitware Inc., and Los Alamos National Laboratory.

U ET AL. 8 of 12

- Andrews-Hanna, J. C., Besserer, J., Head, J. W., III., Howett, C. J. A., Kiefer, W. S., Lucey, P. J., et al. (2014). Structure and evolution of the lunar procellarum region as revealed by grail gravity data. *Nature*, 514(7520), 68–71. https://doi.org/10.1038/nature13697
- Arai, T., Terada, H., Yamaguchi, A., & Ohtake, M. (2008). A new model of lunar crust: Asymmetry in crustal composition and evolution. Earth Planets and Space, 60, 433–444. https://doi.org/10.1186/BF03352808
- Boukaré, C.-E., Parmentier, E. M., & Parman, S. W. (2018). Timing of mantle overturn during magma ocean solidification. *Earth and Planetary Science Letters*, 491(1), 216–225. https://doi.org/10.1016/j.epsl.2018.03.037
- Breuer, D., & Moore, W. (2015). 10.08—Dynamics and thermal history of the terrestrial planets, the Moon, and Io. In G. Schubert (Ed.), *Treatise on geophysics* (2nd ed., pp. 255–305). https://doi.org/10.1016/B978-0-444-53802-4.00173-1
- Cassen, R., & Reynolds, R. T. (1973). Role of convection in the Moon. *Journal of Geophysical Research*, 78(17), 3203–3215. https://doi.org/10.1029/JB078i017p03203
- Cassen, R., Reynolds, R. T., Graziani, F., Summers, A., McNellis, J., & Blalock, L. (1979). Convection and lunar thermal history. *Physics of the Earth and Planetary Interiors*, 19(2), 183–196. https://doi.org/10.1016/0031-9201(79)90082-7
- Charlier, B., Grove, T. L., Namur, O., & Holtz, F. (2018). Crystallization of the lunar magma ocean and the primordial mantle-crust differentiation of the Moon. *Geochimica et Cosmochimica Acta*, 234, 50–69. https://doi.org/10.1016/j.gca.2018.05.006
- Che, X., Nemchin, A., Liu, T., Long, D., Norman, M. D., Joy, K. H., et al. (2021). Age and composition of young basalts on the Moon, measured from samples returned by Chang'e-5. Science, 374(6569), 887–890. https://doi.org/10.1126/science.abl7957
- Cho, Y., Morota, T., Haruyama, J., Yasui, M., Hirata, N., & Sugita, S. (2012). Young mare volcanism in the orientale region contemporary with the procellarum kreep terrane (PKT) volcanism peak period around 2 billion years ago. *Geophysical Research Letters*, 39(11). https://doi.org/10.1029/2012GL051838
- Christensen, U. (1984). Convection with pressure-and temperature-dependent non-Newtonian rheology. *Geophysical Journal International*, 77(2), 343–384. https://doi.org/10.1111/j.1365-246X.1984.tb01939.x
- Clark, J. M., Jaclyn, D. H., Jr., Hiesinger, H., van der Bogert, C. H., & Bernhardt, H. (2017). Investigation of newly discovered lobate scarps: Implications for the tectonic and thermal evolution of the Moon. *Icarus*, 298, 78–88. https://doi.org/10.1016/j.icarus.2017.08.017
- de Vries, J., van den Berg, A., & van Westrenen, W. (2010). Formation and evolution of a lunar core from ilmenite-rich magma ocean cumulates. Earth and Planetary Science Letters, 292(1–2), 139–147. https://doi.org/10.1016/j.epsl.2010.01.029
- Dumoulin, C., Doin, M.-P., & Fleitout, L. (1999). Heat transport in stagnant lid convection with temperature- and pressure-dependent Newtonian or non-Newtonian rheology. *Journal of Geophysical Research*, 104(B6), 12759–12777. https://doi.org/10.1029/1999JB900110
- Dygert, N., Hirth, G., & Liang, Y. (2016). A flow law for ilmenite in dislocation creep: Implications for lunar cumulate mantle overturn. Geophysical Research Letters, 43(2), 532–540. https://doi.org/10.1002/2015GL066546
- Elkins-Tanton, L., Burgess, S., & Yin, Q.-Z. (2011). The lunar magma ocean: Reconciling the solidification process with lunar petrology and geochronology. Earth and Planetary Science Letters, 304(3–4), 326–336. https://doi.org/10.1016/j.epsl.2011.02.004
- Frueh, T., Hiesinger, H., Bogert, C. H., Clark, J. D., Watters, T. R., & Schmedemann, N. (2023). Timing and origin of compressional tectonism in
- mare tranquillitatis. *Journal of Geophysical Research: Planets*, 128, e2022JE007533. https://doi.org/10.1029/2022JE0075 Gagnepain-Beyneix, J., Lognonné, P., Chenet, H., Lombardi, D., & Spohn, T. (2006). A seismic model of the lunar mantle and constraints on
- temperature and mineralogy. *Physics of the Earth and Planetary Interiors*, 159(3–4), 140–166. https://doi.org/10.1016/j.pepi.2006.05.009 Garcia, R. F., Gagnepain-Beyneix, J., Chevrot, S., & Lognonné, P. (2011). Very preliminary reference moon model. *Journal of Geophysical Research*, 188(1–2), 96–113. https://doi.org/10.1016/j.pepi.2011.06.015
- Garcia, R. F., Gagnepain-Beyneix, J., Chevrot, S., & Lognonné, P. (2012). Erratum to "very preliminary reference Moon model". *Physics of the Earth and Planetary Interiors*, 202–203, 89–91. https://doi.org/10.1016/j.pepi.2012.03.009
- Giguere, T. A., Boyce, J. M., Gillis-Davis, J. J., Trang, D., & Stopar, J. D. (2022). Lava flow ages in northeastern oceanus procellarum: The need for calibrating crater counting procedures. *Icarus*, 375, 114838. https://doi.org/10.1016/j.icarus.2021.114838
- Guerrero, J. M., Lowman, J. P., Deschamps, F., & Tackley, P. J. (2018). The influence of curvature on convection in a temperature-dependent viscosity fluid: Implications for the 2-d and 3-d modeling of Moons. *Journal of Geophysical Research: Planets*, 123(7), 1863–1880. https://doi.org/10.1029/2017JE005497
- Haupt, C., Renggli, C., Rohrbach, A., Berndt, J., & Klemme, S. (2024). Experimental constraints on the origin of the lunar high-ti basalts. *Journal of Geophysical Research: Planets*, 129(8), e2023JE008239. https://doi.org/10.1029/2023JE008239
- Head, J. W., & Wilson, L. (2017). Generation, ascent and eruption of magma on the Moon: New insights into source depths, magma supply, intrusions and effusive/explosive eruptions (part 2: Predicted emplacement processes and observations). *Icarus*, 283, 176–223. https://doi.org/10.1016/j.icarus.2016.05.031
- Head, J. W., & Wilson, L. (2020). Magmatic intrusion-related processes in the upper lunar crust: The role of country rock porosity/permeability in magmatic percolation and thermal annealing, and implications for gravity signatures. *Planetary and Space Science*, 180(104765), 104765. https://doi.org/10.1016/j.pss.2019.104765
- Head, J. W., Wilson, L., Hiesinger, H., van der Bogert, C., Chen, Y., Dickson, J. L., et al. (2023). Lunar mare basaltic volcanism: Volcanic features and emplacement processes. Reviews in Mineralogy and Geochemistry, 89(1), 453–507. https://doi.org/10.2138/rmg.2023.89.11
- Hess, P. C., & Parmentier, E. M. (1995). A model for the thermal and chemical evolution of the Moon's interior: Implications for the onset of mare volcanism. Earth and Planetary Science Letters, 134(3-4), 501–514. https://doi.org/10.1016/0012-821X(95)00138-3
- Hiesinger, H., Head, J. W., III., Wolf, U., Jaumann, R., & Neukum, G. (2003). Ages and stratigraphy of mare basalts in oceanus procellarum, mare nubium, mare cognitum, and mare insularum. *Journal of Geophysical Research*, 108(E7), 5065. https://doi.org/10.1029/2002JE001985
- Hiesinger, H., Jaumann, R., Neukum, G., & Head, J. W. (2000). Ages and stratigraphy of mare basalts in oceanus procellarum, mare nubium, mare cognitum, and mare insularum. *Journal of Geophysical Research*, 105(E12), 29239–29275. https://doi.org/10.1029/2000JE001244
- Hirth, G., & Kohlstedt, D. L. (2003). Rheology of the upper mantle and the mantle wedge: A view from the experimentalists. Geophysical Monograph Series, 138, 83–105. https://doi.org/10.1029/138GM06
- Hurwitz, D. M., Head, J. W., & Hiesinger, H. (2013). Lunar sinuous rilles: Distribution, characteristics, and implications for their origin. *Planetary and Space Science*, 79, 1–38. https://doi.org/10.1016/j.pss.2012.10.019
- Jolliff, B. L., Gillis, J. J., Haskin, L. A., Korotev, R. L., & Wieczorek, M. A. (2000). Major lunar crustal terranes: Surface expressions and crustal-mantle origins. *Journal of Geophysical Research*, 105(E2), 4197–4216. https://doi.org/10.1029/1999JE001103
- Jones, M. J., Evans, A. J., Johnson, B. C., Weller, M. B., Andrews-Hanna, J. C., Tikoo, S. M., & T, K. J. (2022). A south pole–aitken impact origin of the lunar compositional asymmetry. Science Advances, 8(14). https://doi.org/10.1126/sciadv.abm8475
- Kamata, S., Sugita, S., Abe, Y., Ishihara, Y., Harada, Y., Morota, T., et al. (2013). Viscoelastic deformation of lunar impact basins: Implications for heterogeneity in the deep crustal paleo-thermal state and radioactive element concentration. *Journal of Geophysical Research: Planets*, 118(3), 398–415. https://doi.org/10.1002/jgre.20056

U ET AL. 9 of 12

- Kato, S., Morota, T., Yamaguchi, Y., Watanabe, S.-I., Otake, H., & Ohtake, M. (2017). Magma source transition of lunar mare volcanism at 2.3 Ga. Meteoritics & Planetary Science, 52(9), 1899–1915. https://doi.org/10.1111/maps.12896
- Katz, R. F. (2008). Magma dynamics with the enthalpy method: Benchmark solutions and magmatic focusing at mid-ocean ridges. Geochemistry, Geophysics, Geosystems, 49(12), 2099–2121. https://doi.org/10.1093/petrology/egn058
- Katz, R. F., Spiegelman, M., & Langmuir, C. H. (2003). A new parameterization of hydrous mantle melting. Geochemistry, Geophysics, Geosystems, 4(9), 1073. https://doi.org/10.1029/2002GC000433
- Khan, A., Connolly, J. A. D., Pommier, A., & Noir, J. (2014). Geophysical evidence for melt in the deep lunar interior and implications for lunar evolution. *Journal of Geophysical Research: Planets*, 119(10), 2197–2221. https://doi.org/10.1002/2014JE004661
- Khan, A., Maclennan, J., Taylor, S. R., & Connolly, J. A. D. (2006). Are the earth and the moon compositionally alike? Inferences on lunar composition and implications for lunar origin and evolution from geophysical modeling. *Journal of Geophysical Research*, 111(E5). https://doi.org/10.1029/2005JE002608
- Kirk, R. L., & Stevenson, D. J. (1989). The competition between thermal contraction and differentiation in the stress history of the Moon. *Journal of Geophysical Research*, 94(B9), 12133–12144. https://doi.org/10.1029/JB094iB09p12133
- Klimczak, C. (2015). Limits on the brittle strength of planetary lithospheres undergoing global contraction. *Journal of Geophysical Research: Planets*, 120(12), 2135–2151. https://doi.org/10.1002/2015JE004851
- Konrad, W., & Spohn, T. (1997). Thermal history of the Moon: Implications for an early core dynamo and post-accertional magmatism. Advances in Space Research, 19(10), 1511–1521. https://doi.org/10.1016/S0273-1177(97)00364-5
- Kronrod, E., Matsumoto, K., Kuskov, O. L., Kronrod, V., Yamada, R., & Kamata, S. (2022). Towards geochemical alternatives to geophysical models of the internal structure of the lunar mantle and core. Advances in Space Research, 69(7), 2798–2824. https://doi.org/10.1016/j.asr. 2022.01.012
- Laneuville, M., Taylor, J., & Wieczorek, M. A. (2018). Distribution of radioactive heat sources and thermal history of the Moon. *Journal of Geophysical Research: Planets*, 123(12), 3144–3166. https://doi.org/10.1029/2018JE005742
- Laneuville, M., Wieczorek, M. A., Breuer, D., Aubert, J., & Ruckriemen, T. (2014). A long-lived lunar dynamo powered by core crystallization. Earth and Planetary Science Letters, 401, 251–260. https://doi.org/10.1016/j.epsl.2014.05.057
- Laneuville, M., Wieczorek, M. A., Breuer, D., & Tosi, N. (2013). Asymmetric thermal evolution of the Moon. *Journal of Geophysical Research: Planets*, 118(7), 1435–1452. https://doi.org/10.1002/jgre.20103
- Lawrence, D. J., Feldman, W. C., Barraclough, B. L., Binder, A. B., Elphic, R. C., Maurice, S., et al. (2000). Small-area thorium features on the lunar surface. *Journal of Geophysical Research*, 105(E8), 20307–20331. https://doi.org/10.1029/1999JE001177
- Le Bars, M., & Davaille, A. (2004). Whole layer convection in a heterogeneous planetary mantle. *Journal of Geophysical Research*, 109(B03403). https://doi.org/10.1029/2003JB002617
- Li, H., Zhang, N., Ling, Y., Wu, B., Dygert, N. K., Huang, J., & Parmentier, E. M. (2019). Lunar cumulate mantle overturn: A model constrained
- by ilmenite rheology. *Journal of Geophysical Research: Planets*, 124(5), 1357–1378. https://doi.org/10.1029/2018JE005905 Li, Q.-L., Zhou, Q., Liu, Y., Xiao, Z., Lin, Y., Li, J.-H., et al. (2021). Two-billion-year-old volcanism on the Moon from Chang'e-5 basalts. *Nature*,
- 600(7887), 54–58. https://doi.org/10.1038/s41586-021-04100-2 Liang, W., & Andrews-Hanna, J. C. (2022). Probing the source of ancient linear gravity anomalies on the Moon. *Icarus*, 380(114978), 114978.
- https://doi.org/10.1016/j.icarus.2022.114978
 Liang, W., Broquet, A., Andrews-Hanna, J. C., Zhang, N., Ding, M., & Evans, A. J. (2024). Vestiges of a lunar ilmenite layer following mantle
- overturn revealed by gravity data. *Nature Geoscience*, 17(4), 361–366. https://doi.org/10.1038/s41561-024-01408-2 Lodders, K. (2003). Solar system abundances and condensation temperatures of the elements. *The Astrophysical Journal*, 591(2), 1220–1247.
- https://doi.org/10.1086/375492 Loper, D. E., & Werner, C. L. (2002). On lunar asymmetries 1. Tilted convection and crustal asymmetry. *Journal of Geophysical Research*,
- 107(E6). https://doi.org/10.1029/2000IE001441
 Lourenço, D. L., Rozel, A. B., Gerya, T., & Tackley, P. J. (2018). Efficient cooling of rocky planets by intrusive magmatism. *Nature Geoscience*,
- 11(5), 322–327. https://doi.org/10.1038/s41561-018-0094-8
- Luo, B., Wang, Z., Song, J., Qian, Y., He, Q., Li, Y., et al. (2023). The magmatic architecture and evolution of the Chang'e-5 lunar basalts. *Nature Geoscience*, 16(4), 301–308. https://doi.org/10.1038/s41561-023-01146-x
- Matsuyama, L., Keane, J. T., Trinh, A., Beuthe, M., & Watters, T. R. (2021). Global tectonic patterns of the Moon. Geophysical Research Letters, 358(114202), 114202. https://doi.org/10.1016/j.icarus.2020.114202
- Maurice, M., Tosi, N., & Hüttig, C. (2024). Small-scale overturn of high-ti cumulates promoted by the long lifetime of the lunar magma ocean. Journal of Geophysical Research: Planets, 129(2), e2023JE008060. https://doi.org/10.1029/2023JE008060
- McDonough, W. F., & Sun, S.-S. (1995). The composition of the Earth. *Journal of Geophysical Research*, 120(3–4), 223–253. https://doi.org/10.1016/0009-2541(94)00140-4
- McKenzie, D. (1984). The generation and compaction of partially molten rock. *Journal of Petrology*, 25(3), 713–765. https://doi.org/10.1093/petrology/25.3.713
- Mei, S., Bai, W., Hiraga, T., & Kohlstedt, D. L. (2002). Influence of melt on the creep behavior of olivine-basalt aggregates under hydrous conditions. Earth and Planetary Science Letters, 201(3-4), 491-507. https://doi.org/10.1016/S0012-821X(02)00745-8
- Miller, K. J., Zhu, W.-L., Montési, L. G. J., & Gaetani, G. A. (2014). Experimental quantification of permeability of partially molten mantle rock. Earth and Planetary Science Letters, 388(15), 273–282. https://doi.org/10.1016/j.epsl.2013.12.003
- Morota, T., Haruyama, J., Honda, C., Ohtake, M., Yokota, Y., Kimura, J., et al. (2009). Mare volcanism in the lunar farside moscoviense region: Implication for lateral variation in magma production of the Moon. *Geophysical Research Letters*, 36(L21202). https://doi.org/10.1029/2009GL040472
- Morota, T., Haruyama, J., Ohtake, M., Matsunaga, T., Honda, C., Yokota, Y., et al. (2011). Timing and characteristics of the latest mare eruption on the Moon. Earth and Planetary Science Letters, 302(3-4), 255–266. https://doi.org/10.1016/j.epsl.2010.12.028
- Nagaoka, H., Fagan, T. J., Kayama, M., Karouji, Y., Hasebe, N., & Ebihara, M. (2020). Formation of ferroan dacite by lunar silicic volcanism recorded in a meteorite from the Moon. *Progress in Earth and Planetary Science*, 7, 1–18. https://doi.org/10.1186/s40645-020-0324-8
- Nishiyama, G., Morota, T., Namiki, N., Inoue, K., & Sugita, S. (2024). Lunar low-titanium magmatism during ancient expansion inferred from ejecta originating from linear gravity anomalies. *Journal of Geophysical Research: Planets*, 129(10), e2023JE008034. https://doi.org/10.1029/2023JE008034
- Noack, L., & Breuer, D. (2013). First-and second-order frank-kamenetskii approximation applied to temperature-pressure-and stress-dependent rheology. *Geophysical Journal International*, 195(1), 27–46. https://doi.org/10.1093/gji/ggt248
- Ogawa, M. (2018a). The effects of magmatic redistribution of heat producing elements on the lunar mantle evolution inferred from numerical models that start from various initial states. *Planetary and Space Science*, 151, 43–55. https://doi.org/10.1016/j.pss.2017.10.015

U ET AL. 10 of 12

- Ogawa, M. (2018b). Magmatic differentiation and convective stirring of the mantle in early planets: The effects of the magmatism-mantle upwelling feedback. *Geophysical Journal International*, 215(3), 2144–2155. https://doi.org/10.1093/gji/ggy413
- Ogawa, M. (2020). Magmatic differentiation and convective stirring of the mantle in early planets—2: Effects of the properties of mantle materials. *Geophysical Journal International*, 220(2), 1409–1420. https://doi.org/10.1093/gji/ggz499
- Parmentier, E. M., Zhong, S., & Zuber, M. T. (2002). Gravitational dijerentiation due to initial chemical strati¢cation: Origin of lunar asymmetry by the creep of dense kreep? *Earth and Planetary Science Letters*, 201(3–4), 473–480. https://doi.org/10.1016/S0012-821X(02)00726-4
- Ringwood, A. E., & Kesson, S. E. (1976). A dynamic model for mare basalt petrogenesis. In *Proceedings of the Lunar Science Conference* (Vol. 7, pp. 1697–1722).
- Rolf, T., Zhu, M.-H., Wünnemann, K., & Werner, S. C. (2017). The role of impact bombardment history in lunar evolution. *Icarus*, 286, 138–152. https://doi.org/10.1016/j.icarus.2016.10.007
- Sakamaki, T., Ohtani, E., Urakawa, S., Suzuki, S., Katayama, Y., & Zhao, D. (2010). Density of high-ti basalt magma at high pressure and origin of heterogeneities in the lunar mantle. Earth and Planetary Science Letters, 299(3–4), 285–289. https://doi.org/10.1016/j.epsl.2010.09.007
- Sato, H., Robinson, M. S., Lawrence, S. J., Denevi, B. W., Hapke, B., Jolliff, B. L., & Hiesinger, H. (2017). Lunar mare Tio2 abundances estimated from UV/VIS reflectance. *Icarus*, 296, 216–238. https://doi.org/10.1016/j.icarus.2017.06.013
- Sawada, N., Morota, T., Kato, S., Ishihara, Y., & Hiramatsu, Y. (2016). Constraints on timing and magnitude of early global expansion of the Moon from topographic features in linear gravity anomaly areas. Geophysical Research Letters, 43(10), 4865–4870. https://doi.org/10.1002/ 2016GL068966
- Schwinger, S., & Breuer, D. (2022). Employing magma ocean crystallization models to constrain structure and composition of the lunar interior. Physics of the Earth and Planetary Interiors, 322, 106831. https://doi.org/10.1016/j.pepi.2021.106831
- Scott, T., & Kohlstedt, D. L. (2006). The effect of large melt fraction on the deformation behavior of peridotite. *Geophysical Monograph Series*, 246(3–4), 177–187, https://doi.org/10.1016/j.epsl.2006.04.027
- Shearer, C. K., Hess, P. C., Wieczorek, M. A., Pritchard, M. E., Parmentier, E. M., Borg, L. E., et al. (2006). Thermal and magmatic evolution of the Moon. *Reviews in Mineralogy and Geochemistry*, 60(1), 365–518. https://doi.org/10.2138/rmg.2006.60.4
- Snyder, G. A., Taylor, L. A., & Neal, C. R. (1992). A chemical model for generating the sources of mare basalts: Combined equilibrium and fractional crystallization of the lunar magmasphere. Geochimica et Cosmochimica Acta, 56(10), 3809–3823. https://doi.org/10.1016/0016-7037(92)90172-F
- Solomon, S. C., & Chaiken, J. (1976). Thermal expansion and thermal stress in the Moon and terrestrial planets: Clues to early thermal history. In *Proceedings of the Lunar Science Conference* (Vol. 7, pp. 3229–3243).
- Solomon, S. C., & Head, J. W. (1979). Vertical movement in mare basins: Relation to mare emplacement, basin tectonics, and lunar thermal history. *Journal of Geophysical Research*, 84(B4), 1667–1682. https://doi.org/10.1029/JB084iB04p01667
- Solomon, S. C., & Toksöz, M. N. (1973). Internal constitution and evolution of the Moon. *Physics of the Earth and Planetary Interiors*, 7(1), 15–38. https://doi.org/10.1016/0031-9201(73)90037-X
- Spohn, T., Konrad, W., Breuer, D., & Ziethe, R. (2001). The longevity of lunar volcanism: Implications of thermal evolution calculations with 2d and 3d mantle convection models. *Icarus*, 149(1), 54–65. https://doi.org/10.1006/icar.2000.6514
- Stegman, D. R., Jellinek, A. M., Zatman, S. A., Baumgardner, J. R., & Richards, M. A. (2003). An early lunar core dynamo driven by thermochemical mantle convection. *Nature*, 421(6919), 143–146. https://doi.org/10.1038/nature01267
- Su, B., Yuan, J., Chen, Y., Yang, W., Mitchell, R. N., Hui, H., et al. (2022). Fusible mantle cumulates trigger young mare volcanism on the cooling Moon. Science Advances. 8(42). https://doi.org/10.1126/sciady.abn2103
- Taguchi, M., Morota, T., & Kato, S. (2017). Lateral heterogeneity of lunar volcanic activity according to volumes of mare basalts in the farside basins. *Journal of Geophysical Research: Planets*, 122(7), 1505–1521. https://doi.org/10.1002/2016JE005246
- Taylor, G. J., & Wieczorek, M. A. (2014). Lunar bulk chemical composition: A post-gravity recovery and interior laboratory reassessment. Philosophical Transactions of the Royal Society A, 372(2024), 20130242. https://doi.org/10.1098/rsta.2013.0242
- Tian, H.-C., Zhang, C., Yang, W., Du, J., Chen, Y., Xiao, Z., et al. (2023). Surges in volcanic activity on the Moon about two billion years ago. *Nature Communications*, 14(1), 3734. https://doi.org/10.1038/s41467-023-39418-0
- Turcotte, D. L., & Schubert, G. (2014). Geodynamics. Cambridge University Press. https://doi.org/10.1017/CBO9780511843877
- U, K., Hasumi, H., & Ogawa, M. (2022). Effects of magma-generation and migration on the expansion and contraction history of the Moon. *Earth Planets and Space*, 74(78), 78. https://doi.org/10.1186/s40623-022-01631-4
- U, K., Kameyama, M., Gaku, N., Miyagoshi, T., & Ogawa, M. (2024). Numerical models of magmatism in the convective mantle of the Moon 2: Role for localized radioactive enrichment Dataset. Figshare. https://doi.org/10.6084/m9.figshare.26135734
- U, K., Kameyama, M., & Ogawa, M. (2023a). Numerical models of magmatism in the convective mantle of the Moon Dataset. Figshare. https://doi.org/10.6084/m9.figshare.22297921
- U, K., Kameyama, M., & Ogawa, M. (2023b). The volcanic and radial expansion/contraction history of the Moon simulated by numerical models of magmatism in the convective mantle. *Journal of Geophysical Research: Planets*, 128(e2023JE007845). https://doi.org/10.1029/ 2023JE007845
- van der Bogert, C. H., Clark, J. D., Hiesinger, H., Banks, M. E., Watters, T. R., & Robinson, M. S. (2018). How old are lunar lobate scarps? 1. Seismic resetting of crater size-frequency distributions. *Icarus*, 306, 225–242. https://doi.org/10.1016/j.icarus.2018.01.019
- van Kan Parker, M., Sanloup, C., Sator, N., Guillot, B., Tronche, E. J., Perrillat, P., et al. (2012). Neutral buoyancy of titanium-rich melts in the deep lunar interior. *Nature Geoscience*, 5(3), 186–189. https://doi.org/10.1038/ngeo1402
- Wasson, J. T., & Warren, P. H. (1980). Contribution of the mantle to the lunar asymmetry. *Icarus*, 44(3), 752–771. https://doi.org/10.1016/0019-1035(80)90142-6
- Watters, T. R., Robinson, M. S., Beyer, R. A., Banks, M. E., Bell, J. F., Pritchard, M. E., et al. (2010). Evidence of recent thrust faulting on the Moon revealed by the lunar reconnaissance orbiter camera. *Science*, 329(5994), 936–940. https://doi.org/10.1126/science.1189590
- Watters, T. R., Robinson, M. S., Collins, G. C., Banks, M. E., Daud, K., Williams, N. R., & Selvans, M. M. (2015). Global thrust faulting on the Moon and the influence of tidal stresses. *Geology*, 43(10), 851–854. https://doi.org/10.1130/G37120.1
- Whitehead, J. A. (1988). Fluid models of geological hotspots. Annual Review of Fluid Mechanics, 20(1), 61–87. https://doi.org/10.1146/annurev.fl.20.010188.000425
- Whitten, J. L., & Head, J. W. (2015). Lunar cryptomaria: Physical characteristics, distribution, and implications for ancient volcanism. *Icarus*, 247, 150–171. https://doi.org/10.1016/j.icarus.2014.09.031
- Wieczorek, M. A., Neumann, G. A., Nimmo, F., Kiefer, W. S., Taylor, G. J., Melosh, R. J., et al. (2013). The crust of the Moon as seen by grail. Science, 339(6029), 671–675. https://doi.org/10.1126/science.1199375
- Wieczorek, M. A., & Phillips, R. J. (2000). The "procellarum kreep terrane": Implications for mare volcanism and lunar evolution. *Journal of Geophysical Research*, 105(E8), 20417–20430. https://doi.org/10.1029/1999JE001092

U ET AL. 11 of 12

- Wilson, L., & Head, J. W. (2003). Deep generation of magmatic gas on the Moon and implications for pyroclastic eruptions. *Icarus*, 30(12). https://doi.org/10.1029/2002GL016082
- Wilson, L., & Head, J. W. (2017). Generation, ascent and eruption of magma on the Moon: New insights into source depths, magma supply, intrusions and effusive/explosive eruptions (part 1: Theory). *Icarus*, 283, 146–175. https://doi.org/10.1016/j.icarus.2015.12.039
- Wood, J. A. (1972). Thermal history and early magmatism in the Moon. *Icarus*, 16(2), 229–240. https://doi.org/10.1016/0019-1035(72)90070-X Xu. M., Jing, Z., Van Orman, J. A., Yu. T., & Wang, Y. (2022). Experimental evidence supporting an overturned iron-titanium-rich melt layer in
- Xu, M., Jing, Z., Van Orman, J. A., Yu, T., & Wang, Y. (2022). Experimental evidence supporting an overturned iron-titanium-rich melt layer in the deep lunar interior. *Geophysical Research Letters*, 49(13). https://doi.org/10.1029/2022GL099066
- Yanagisawa, T., Kameyama, M., & Ogawa, M. (2016). Numerical studies on convective stability and flow pattern in three-dimensional spherical mantle of terrestrial planets. *Geophysical Journal International*, 206(3), 1526–1538. https://doi.org/10.1093/gji/ggw226
- Yu, S., Tosi, N., Schwinger, S., Maurice, M., Breuer, D., & Xiao, L. (2019). Overturn of ilmenite-bearing cumulates in a rheologically weak lunar mantle. *Journal of Geophysical Research: Planets*, 124(2), 418–436. https://doi.org/10.1029/2018je005739
- Yue, Z., Michael, G. G., Di, K., & Liu, J. (2017). Global survey of lunar wrinkle ridge formation times. Earth and Planetary Science Letters, 477, 14–20. https://doi.org/10.1016/j.epsl.2017.07.048
- Zhang, D., Su, B., Chen, Y., Yang, W., Mao, Q., & Jia, L.-H. (2022). Titanium in olivine reveals low-ti origin of the Chang'e-5 lunar basalts. Lithos, 414, 106639. https://doi.org/10.1016/j.lithos.2022.106639
- Zhang, N., Ding, M., Zhu, M.-H., Li, H., Li, H., & Yue, Z. (2022). Lunar compositional asymmetry explained by mantle overturn following the
- south pole–aitken impact. *Nature Geoscience*, 15(1), 37–41. https://doi.org/10.1038/s41561-021-00872-4

 Zhang, N., Dygert, N., Liang, Y., & Parmentier, E. (2017). The effect of ilmenite viscosity on the dynamics and evolution of an overturned lunar cumulate mantle. *Geophysical Research Letters*, 44(13), 6543–6552. https://doi.org/10.1002/2017GL073702
- Zhang, N., Parmentier, E., & Liang, Y. (2013a). A 3-d numerical study of the thermal evolution of the moon after cumulate mantle overturn: The importance of rheology and core solidification. *Journal of Geophysical Research: Planets*, 118(9), 1789–1804. https://doi.org/10.1002/jgre.
- Zhang, N., Parmentier, E., & Liang, Y. (2013b). Effects of lunar cumulate mantle overturn and megaregolith on the expansion and contraction history of the Moon. *Geophysical Research Letters*, 40(19), 5019–5023. https://doi.org/10.1002/grl.50988
- Zhang, W., Zhang, N., & Li, H. Y. (2022). Abundances of lunar heat-producing elements constrained by a 3-d numerical model of titanium-rich basaltic eruption. Chinese Journal of Geophysics, 65(1), 119–136. https://doi.org/10.6038/cjg2022P0753
- Zhang, W., Zhang, N., Liang, Y., & Tokle, L. (2023). The effect of pressure-dependent viscosity on the dynamics of the post-overturn lunar mantle. *Journal of Geophysical Research: Planets*, 128(10), e2023JE007933. https://doi.org/10.1029/2023JE007933
- Zhao, Y., de Vries, J., van den Berg, A. P., Jacobs, M. H. G., & van Westrenen, W. (2019). The participation of ilmenite-bearing cumulates in lunar mantle overturn. Earth and Planetary Science Letters, 511(1), 1–11. https://doi.org/10.1016/j.epsl.2019.01.022
- Zhong, S., Parmentier, E. M., & Zuber, M. T. (2000). A dynamic origin for the global asymmetry of lunar mare basalts. *Earth and Planetary Science Letters*, 177(3-4), 131–140. https://doi.org/10.1016/S0012-821X(00)00041-8
- Zhu, M.-H., Wünnemann, K., Potter, R. W., Kleine, T., & Morbidelli, A. (2019). Are the Moon's nearside-farside asymmetries the result of a giant impact? *Journal of Geophysical Research: Planets*, 124(8), 2117–2140. https://doi.org/10.1029/2018JE005826
- Ziethe, R., Seiferlin, K., & Hiesinger, H. (2009). Duration and extent of lunar volcanism: Comparison of 3d convection models to mare basalt ages. *Planetary and Space Science*, 57(7), 784–796. https://doi.org/10.1016/j.pss.2009.02.002

References From the Supporting Information

- Christensen, U. R., Holzwarth, V., & Reiners, A. (2009). Energy flux determines magnetic field strength of planets and stars. *Nature*, 457(7226), 167–169. https://doi.org/10.1038/nature07626
- Jung, J.-I., Tikoo, S. M., Burns, D., Váci, Z., & Krawczynski, M. J. (2024). Assessing lunar paleointensity variability during the 3.9-3.5 Ga high field epoch. Earth and Planetary Science Letters, 638, 118757. https://doi.org/10.1016/j.epsl.2024.118757
- Karato, S. (2013). Geophysical constraints on the water content of the lunar mantle and its implications for the origin of the Moon. Earth and Planetary Science Letters, 384, 144–153. https://doi.org/10.1016/j.epsl.2013.10.001
- Siegler, M. A., & Smrekar, S. E. (2014). Lunar heat flow: Regional prospective of the apollo landing sites. *Journal of Geophysical Research: Planets*, 119(1), 47–63. https://doi.org/10.1002/2013JE004453
- Siegler, M. A., Warren, P., Franco, K. L., Paige, D., Feng, J., & White, M. (2022). Lunar heat flow: Global predictions and reduced heat flux. Journal of Geophysical Research: Planets, 127(9), e2022JE007182. https://doi.org/10.1029/2022JE007182
- Tarduno, J. A., Cottrell, R. D., Lawrence, K., Bono, R. K., Huang, W., Johnson, C. L., et al. (2021). Absence of a long-lived lunar paleo-magnetosphere. Science Advances, 7(32), eabi7647. https://doi.org/10.1126/sciadv.abi7647
- Tikoo, S. M., Weiss, B. P., Shuster, D. L., Suavet, C., Wang, H., & Grove, T. L. (2017). A two-billion-year history for the lunar dynamo. *Science Advances*, 3(8), e1700207. https://doi.org/10.1126/sciadv.1700207
- Weiss, B. P., & Tikoo, S. M. (2014). The lunar dynamo. Science, 346(6214), 1246753. https://doi.org/10.1126/science.1246753

U ET AL. 12 of 12